Phys Chem Minerals (2012) 39:87–92
DOI 10.1007/s00269-011-0463-y

ORIGINAL PAPER

Magnetic thermodynamics as proxy for chemical inhomogeneity in hemo-ilmenite solid solutions

A dynamic *ac* susceptibility study

M. Charilaou · J. F. Löffler · A. U. Gehring

Received: 9 May 2011 / Accepted: 20 September 2011 / Published online: 7 October 2011

Abstract In this study, we present *ac* susceptibility measurements for a synthetic and a natural hemo-ilmenite (HI) solid solution $(x)FeTiO_3$–$(1 - x)Fe_2O_3$ with compositions $x = 0.87(1)$ and 0.88(8), respectively. The focus of the investigation is the magnetic ordering at the Curie temperature T_C and the spin-glass-like freezing at the freezing temperature T_f. The sharpness of T_C for the synthetic solid solution with well-defined structure indicates the chemical homogeneity of the solution, whereas the disperse magnetic ordering of the natural solid solution reveals inhomogeneities described as spin glass system ofvariations in composition x. The frequency dispersion of T_f was determined between 10 Hz and 10 kHz and was found to obey a dynamic scaling power law. The relaxation rates deviate by five orders of magnitude where the synthetic solid solution exhibits $\omega_0 = 3(1) \times 10^4$ Hz and the natural one 5.5×10^9 Hz. The strong deviation is attributed to the difference in the ordered state above T_f. These findings provide an insight into the cooling-rate effects of natural solid solutions and how magnetic thermodynamics can be used to probe the chemical homogeneity of such systems.

Keywords Hemo-ilmenite · Chemical inhomogeneity · Magnetic ordering · Spin-glass-like freezing

M. Charilaou (✉) · A. U. Gehring
Department of Earth Sciences, Institute of Geophysics, ETH Zurich, 8092 Zurich, Switzerland
e-mail: michalis.charilaou@erdw.ethz.ch

J. F. Löffler
Department of Materials, Laboratory of Metal Physics and Technology, ETH Zurich, 8093 Zurich, Switzerland

Introduction

The hemo-ilmenite (HI) solid solution series $(x)FeTiO_3$–$(1 - x)Fe_2O_3$ has attracted increasing interest in solid-state physics and Earth sciences due to its complex magnetic phase diagram and natural occurrence. In a petrological context, the solid solution has been used as thermo-oxy-barometer for the reconstruction of processes in the Earth's crust (Lindsley 1963; Sauerzapf et al. 2008).

The solid solution orders either in the $R\bar{3}$ or in the $R\bar{3}c$ symmetry when Fe(III) enters the lattice, where the Fe(II) and Ti(IV) are partitioned into planes or distributed randomly, respectively. The solid solution is stable above $T > 1{,}000$ K, and the transition temperature from $R\bar{3}c$ to $R\bar{3}$ is a function of the composition (Harrison et al. 2000). Quenching during fast-ascent eruptions forms chemically homogeneous solid solutions. Slow cooling in intrusive systems and slow-ascent eruption with magma stagnation in shallow domes generate the formation of exsolutions, e.g., fine-structured lamellae (McEnroe et al. 2007). The chemistry and texture of HI in geological systems is determined mainly by the cooling rate, which can vary from a few degrees per hour to a few degrees per millions of years. Therefore, the system stores geological information in its structure, which can in turn be used to constrain cooling rates or temperature variations. The structure and texture characterization usually proceeds via transmission electron microscopy or microprobe analysis, which does not probe the bulk properties of the sample. Such limitations can, however, be overcome by magnetic characterization.

The solid solution orders as a ferrimagnet for $x > 0.5$ and as antiferromagnet for $x < 0.5$ with an ordering temperature that changes nearly linearly with the composition

(Ishikawa 1962; Burton et al. 2008; Engelmann et al. 2010). At low temperature ($T < 50$ K), the solid solution exhibits characteristic spin-glass-like freezing for $0.6 < x < 0.95$. The spin-glass-like freezing was originally studied by Ishikawa et al. (1983, 1985), Arai and Ishikawa (1985) and Arai et al. (1985a, b) and has been observed in synthetic (Burton et al. 2008; Charilaou et al. 2011a) and natural samples (Gehring et al. 2007, 2008) in recent studies. It was originally proposed by Ishikawa et al. (1985) that HIs with compositions $x > 0.8$ form Fe(III)-rich clusters. Recently, ferromagnetic resonance and Mössbauer spectroscopy experiments at low temperature provided further evidence that such clusters may exist in the system (Gehring et al. 2008; Frandsen et al. 2010). The presence of clustered Fe(III) alters the chemical homogeneity of the solid solution and thus strongly affects the magnetic thermodynamics of the system.

With this in mind, thermodynamic phenomena such as ordering or freezing are best studied by measuring the dynamic *ac* susceptibility $\chi(T)$, which consists of the in-phase component $\chi'(T)$ and the out-of-phase component $\chi''(T)$. The in-phase component is the fundamental susceptibility, and the out-of-phase component describes dissipation effects and is therefore an excellent proxy for the detection of magnetic phase transitions. The ordering temperature of the solid solution can be detected as a divergence of $\chi''(T)$ upon cooling, which is caused by the onset of hysteretic effects (Rüdt et al. 2004). In a perfect ferro- or ferrimagnet, the ordering is a singularity, and the divergence of $\chi''(T)$ is expected to describe a delta function. In real systems, however, anisotropy mechanisms and chemical inhomogeneities result in a broadening of the divergence below T_C. The spin-glass-like freezing of the system at low temperature ($T < 50$ K) can also be determined using $\chi''(T)$, which exhibits a Lorentzian-like peak at freezing temperature T_f (Charilaou et al. 2011b). In addition, T_f depends strongly on the frequency at which it is measured, typical of thermal activation processes. The frequency dispersion can therefore provide additional information about the internal structure of the solid solution.

In this study, we investigate in detail the magnetic ordering and the dynamics of the spin-glass-like freezing of two samples: a natural and a synthetic HI solid solution of similar composition. In contrast to the synthetic samples, the genesis of the detrital HI particles in the natural samples is not known. The experimental results and the analysis of the freezing dynamics are presented and provide an insight into the freezing mechanisms of dilute and clustered solid solutions. Finally, the freezing properties of the HIs are discussed in the context of the geological origin of the natural particles.

Samples and methods

The synthetic solid solution was fabricated by solid-oxide reaction between the end-members at 1,400 K for 48 h in a protective Ar atmosphere and was quenched in water. The natural HI particles are residual products in a soil from a flood plain in southern Mali (Gehring et al. 1997). The mineral composition of the sample was determined by X-ray diffraction (XRD). The magnetic measurements were taken on untreated bulk samples and after treatment with HCl in order to selectively remove magnetite (Gehring et al. 2007). The effectiveness of the HCl treatment was checked by magnetization analysis. The dynamic *ac* susceptibility was measured in a Quantum Design Physical Property Measurement System (PPMS) with a driving field amplitude of $H_{ac} = 10$ Oe and a frequency range of 10 Hz to 10 kHz, using logarithmic steps. For exact determination of the freezing temperature, the susceptibility was measured at 0.5 K steps from 10 to 300 K at 1 kHz with $H_{ac} = 10$ Oe.

Results and discussion

The XRD data of the synthetic sample indicate single-phase solid solution, and Rietveld analysis reveals ordering in the $R\bar{3}$ symmetry (Charilaou et al. 2011b). The natural samples consist of clay minerals, quartz, and feldspar as detected by XRD. Magnetite and HI in the samples were below the detection limits of XRD and were only detected by magnetic measurements. In contrast to the untreated sample, the magnetization measurements at room temperature of the HCl-treated samples exhibited no phase carrying a remanence, which indicates that all magnetite was removed. Figure 1 shows the normalized in-phase $\chi'(T)$ and out-of-phase component $\chi''(T)$ of the susceptibility $\chi(T)$ for (a) the synthetic and (b) the natural HI after HCl treatment. For the synthetic sample, $\chi'(T)$ shows a paramagnetic-like increase upon cooling from 300 K and exhibits a strong peak at around 130 K. Upon further cooling, $\chi'(T)$ decreases strongly, and at around 40 K, it shows an additional onset of reduction indicating spin-glass-like freezing. The out-of-phase component $\chi''(T)$ is zero upon cooling from high temperature, and at 145 K, it exhibits a steep increase, revealing an ordering of the ferrimagnetic structure at T_C. The ordering is well defined (see inset in Fig. 1a), implying the homogeneity of the solid solution. The ordering temperature of 145 K corresponds to a composition of $x = 0.87(1)$ for the solid solution (Engelmann et al. 2010). Upon further cooling, $\chi''(T)$ reduces to zero again, and at the freezing temperature T_f, it exhibits another peak, which is much lower in intensity than the peak at the ordering.

For the natural solid solution, the in-phase component steadily increases upon cooling and exhibits a pronounced increase below 150 K and a well-defined peak at about 41 K. Upon further cooling, $\chi'(T)$ decreases strongly with a tail below 25 K, which is due to paramagnetic clay minerals in the matrix of the natural sample. The in-phase susceptibility of the untreated samples reveals the same features at low temperature, indicating that magnetite has no effect on the dynamics of the low-temperature susceptibility. The out-of-phase component is close to zero at high temperatures and increases slightly upon cooling, pointing to dispersed ordering. At 130 K, however, it shows a strong increase (see inset in Fig. 1b), which defines the Curie temperature T_C of the solid solution. Upon further cooling, $\chi''(T)$ reaches a plateau between 100 and 50 K, and below 50 K, it exhibits a strong characteristic peak, indicating the spin-glass-like freezing of the system at the freezing temperature T_f. Although the ordering is quite dispersed, the effective ordering temperature of 130 K allows us to extract an effective composition of $x \approx 0.88$ according to Engelmann et al. (2010), which is higher than that estimated based on structural data for this sample (Gehring et al. 2008). However, above T_C, there is a nonzero offset of $\chi''(T)$, which indicates the chemical inhomogeneity in the natural HI and suggests a distribution of compositions among, or inside, the HI grains. This in turn suggests the presence of Fe(III)-richer regions, which order at temperatures well above 130 K, and Fe(III)-deficient regions with an ordering temperature close to that of the end-member ilmenite, as seen from $\chi'(T)$. Despite these inhomogeneities, the effective composition of $x \approx 0.88$ obtained using the magnetic ordering is representative of the system, because the onset of $\chi''(T)$ at 130 K corresponds to the averaged bulk of the sample. We may also estimate the width of the compositional distribution to be $\Delta x = 0.08$.

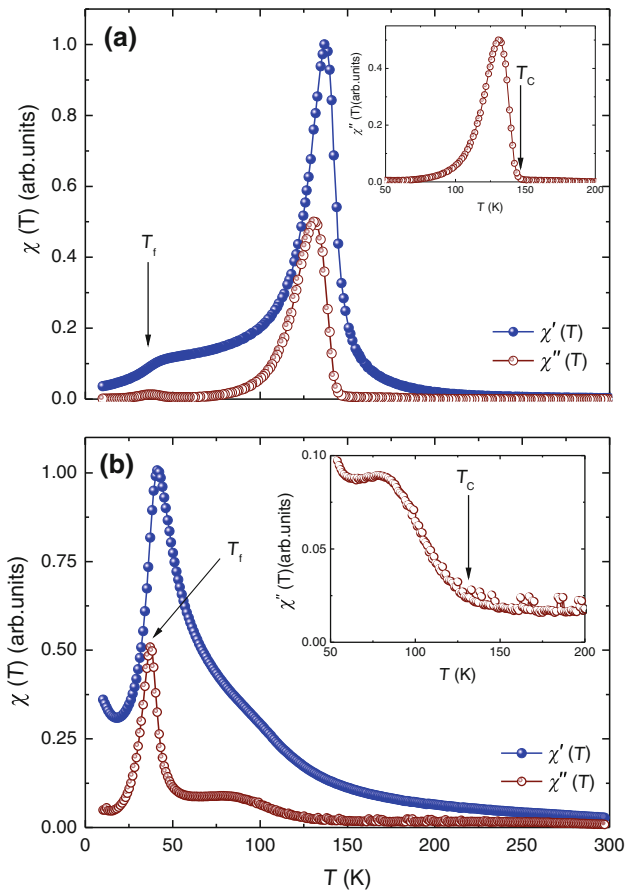

Fig. 1 Normalized *ac* susceptibility of **a** synthetic and **b** natural hemo-ilmenite (HI) with in-phase $\chi'(T)$ (*spheres*) and out-of-phase $\chi''(T)$ (*hollow spheres*) components showing ordering at T_C and freezing at T_f. The *inset* shows a blow-up of the out-of-phase component between 50 and 200 K, indicating the onset of order for the respective sample

The comparison of the $\chi''(T)$ temperature spectra of the two samples reveals a striking difference between the relative intensities at T_C and T_f. For the synthetic sample, the peak at the magnetic ordering is about 40 times stronger than the peak at T_f, whereas for the natural sample, the peak at T_C is 5 times smaller than the peak at T_f. We again attribute this observation to the disperse ordering: While the ordering temperature for compositions $x = 1.0$ to $x = 0.8$ varies by 200 K, the freezing temperature only varies by 10 K. Therefore, all compositions present in the natural sample contribute to a superposition of the peaks at T_f, whereas the opposite takes place for the ordering, where the peak is spread across 200 K in the temperature axis. A contribution of orientation effects to the peak/hight ratio can be excluded because that effect would have the same impact on both ordering and freezing peaks and would therefore be canceled out in the ratio.

The well-defined peak in the $\chi''(T)$ component of the susceptibility at T_f makes possible a detailed investigation of the dynamics of freezing. Figure 2a shows $\chi''(T)$ of the synthetic sample measured at 100 Hz, 1.0 kHz, and 10.0 kHz, whereas Fig. 2b shows the same measurement for the natural solid solution. The exact T_f can be determined at the center of the peak, which is easily defined at the zero-crossing of the derivative $d\chi''(T)/dT$. As can be seen in Fig. 2, T_f is shifted to higher temperatures for higher measurement frequencies in both samples, typical of thermal activation effects. There are, however, two major differences between the temperature spectra of the natural and the synthetic solid solutions: (1) The shift of T_f is much smaller for the natural sample, indicating faster dynamics; and (2) the $\chi''(T)$ peak becomes sharper with increasing frequency for the natural sample, whereas for the synthetic sample, it follows the opposite trend, i.e., becomes broader with increasing frequency.

The width of the $\chi''(T)$ peak indicates the spectrum of relaxation times in the material: At a given frequency ω,

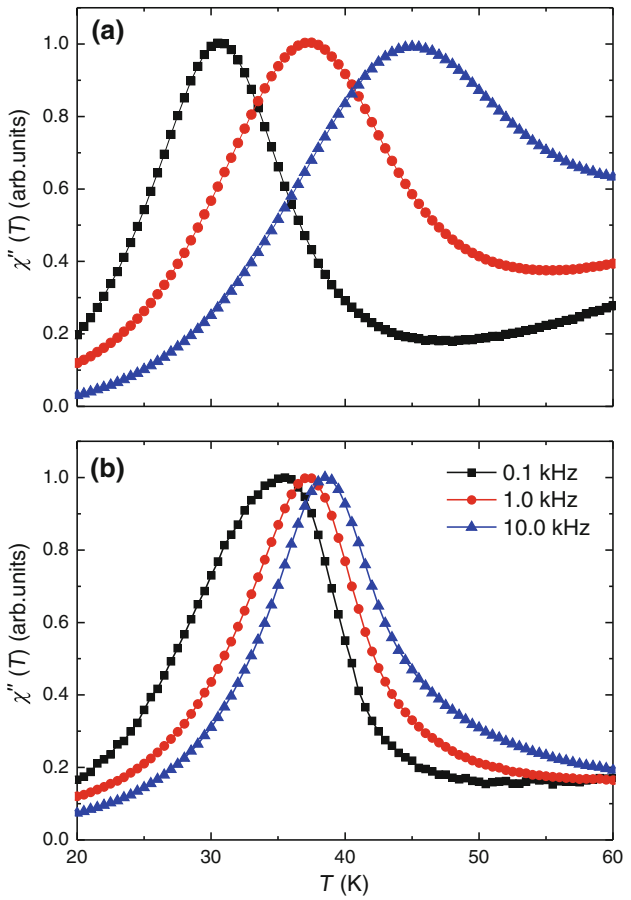

Fig. 2 Out-of-phase component $\chi''(T)$ showing the spin-glass-like freezing in **a** the synthetic and **b** the natural solid solution at 0.1 kHz (*squares*), 1.0 kHz (*circles*), and 10 kHz (*triangles*)

the majority of spins will freeze at T_f, and depending on the inhomogeneity of the structure, other parts of the system will freeze at $T_f(\omega) \pm \Delta T_f(\omega)$, whereas $\Delta T_f(\omega)$ is the linewidth of the peak, which is also frequency dependent. This is also reflected in the profile of the absorption peak, where the high-temperature tail exhibits more asymmetry than the low-temperature one, for both samples, and thus suggests a broader relaxation time distribution at higher temperatures. This variation of relaxation with temperature prevents the description of the frequency dispersion with often utilized Arrhenius- or Vogel-Fulcher-type dynamics, since both phenomenologies assume constant relaxation over the whole temperature spectrum.

The variation of relaxation time with temperature, however, can be well described by the dynamic scaling power law of mean-field theory Ising spin-glasses, which describes a critical slowing down (Hohenberg and Halperin 1977; Binder and Young 1984; Souletie and Tholence 1985; Ogielski and Morgenstern 1985), via

$$\omega = \omega_0 \left(\frac{T_f(\omega)}{T_f} - 1 \right)^{zv}, \qquad (1)$$

where ω is the measurement frequency, ω_0 is a parameter associated with the intrinsic relaxation rate, $T_f(\omega)$ is the freezing temperature at the specific measurement frequency, and T_f is the static (intrinsic) freezing temperature. The dynamic exponent zv is the product of the critical exponent v for the coherence length ξ, which diverges at the freezing temperature with ξ^v, and the dynamic exponent z, which relates the relaxation time to the coherence length with $\tau \propto \xi^z$ (Djurberg et al. 1997; Mauger et al. 1988).

As seen in Fig. 3, both datasets can be fitted nicely using the power law of Eq. 1). It is evident from the data that the freezing temperature range is relatively sharp for the natural and very broad for the synthetic sample. In order to achieve a qualitative description of the data from the fit, we keep the dynamic exponent constant for both samples at $zv = 7(1)$, which is the known value for the 3D Ising spin-glass (Ogielski and Morgenstern 1985), since the HI solid solution represents a typical Ising system (Harrison 2009). Therefore, the fit parameters are the intrinsic freezing temperature T_f and ω_0. By fitting the data, the intrinsic freezing temperatures were found at 33(1) K for the natural and 22(1) K for the synthetic sample. In addition, the relaxation rate for the natural sample was found to be $5.5(2) \times 10^9$ Hz, whereas for the synthetic sample, the value is $3(1) \times 10^4$ Hz. This striking deviation of five orders of magnitude is quite surprising, considering that both samples have similar compositions, i.e., Fe(II)/Fe(III) ratios. Although different compositions are expected to exhibit different relaxation frequencies, this large deviation cannot be attributed to compositional variations.

The discrepancy in the relaxation rates can be reconciled by considering the magnetic state above T_f. The synthetic

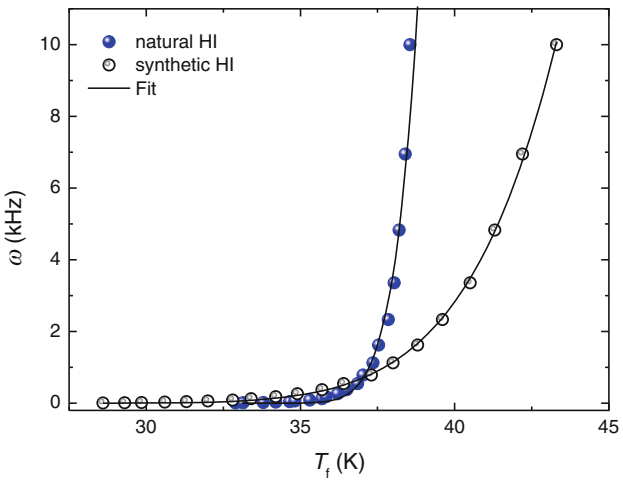

Fig. 3 Frequency dispersion of the freezing temperature T_f for natural HI (*spheres*) and synthetic HI solid solution (*hollow spheres*). *Solid lines* are fits using Eq. 1

solid solution is in a homogeneous state with long-range ordering, as opposed to the disperse ordering in the natural sample. A disperse ordering suggests a variation in the correlation length ξ in the sample, whereas long-range order demands $\xi >> 1$ (here 1 refers to lattice site units). In the synthetic solid solution, the thermal fluctuations therefore occur in collective flipping of spins, i.e., in a superspin manner (Charilaou et al. 2011b), as opposed to single-spin flipping in the natural solid solution. Considering that the rate of thermal fluctuations is $\omega \propto \exp(-E/k_B T)$, where E is the energy barrier, the relaxation rate will decrease with increasing E, which is, in turn, associated with the correlation length, because E increases with increasing superspin size (i.e., correlation length). Therefore, we attribute the large deviation of relaxation rates to the difference in correlation lengths in the synthetic and natural solid solutions.

The absence of well-defined long-range order in the natural solid solution can be attributed to the chemical inhomogeneity in the material, which is probably manifested in a form of clustering. Such inhomogeneities can appear in naturally occurring solid solutions depending on the cooling rate of the material. In contrast, the synthetic solid solution is rapidly quenched from 1,400 K, thus preventing the formation of any effective inhomogeneity.

Finally, the inhomogeneity in the natural samples can be discussed in a geological context. The degree of chemical inhomogeneity in HI reflects its cooling history. The absence of clusters in the quenched synthetic samples provides evidence that fast cooling within seconds generates a solid solution that is homogeneous on the Å-scale. In geological systems, cooling rates are lowered by orders of magnitude even during fast-ascent eruptions. Therefore, based on thermodynamic considerations, homogeneous solid solutions on the Å-scale are unlikely to be formed. However, the formation of inhomogeneities on a molecular level in our natural samples is indicative of fast-cooling processes, by which cation ordering generates an inhomogeneous magnetic pattern but does not form mineral chemical exsolution textures.

Conclusions

We performed dynamic *ac* susceptibility measurements on a natural HI solid solution with effective composition $x = 0.88$ and on a synthetic solution with $x = 0.87$. Both solid solutions exhibit spin-glass-like freezing at low temperature $T < 50$ K with a peak in the out-of-phase component of the susceptibility $\chi''(T)$. Analysis of the freezing dynamics using a power law for dynamic scaling yields relaxation rates that vary by five orders of magnitude. For the natural sample, we obtain $\omega_0 = 5.5 \times 10^9$ Hz, whereas for the synthetic sample, we obtain $\omega_0 = 3(1) \times 10^4$ Hz. We attribute this strong deviation to the chemical inhomogeneity on a molecular level in the natural solid solution, which generates a reduction in the correlation length. These findings clearly show that magnetic thermodynamics can overcome the limitations of structural and textural analysis in detecting inhomogeneities on a molecular level. Moreover, such information for solid solutions can help constrain cooling processes in the Earth's crust, based on the chemical inhomogeneities of the solid solutions.

Acknowledgments The authors would like to thank E. Fischer for his assistance in the sample preparation process. This work was supported by the Swiss National Science Foundation via Grant No. 200021-121844.

References

Arai M, Ishikawa Y (1985a) A new oxide spin glass system of $(1 - x)FeTiO_3 x Fe_2O_3$. III. Neutron scattering studies of magnetization processes in a cluster type spin glass of $90FeTiO_3 10Fe_2O_3$. J Phys Soc Jpn 54:795

Arai M, Ishikawa Y, Saito N, Takei H (1985b) A new oxide spin glass system of $(1 - x)FeTiO_3 x Fe_2O_3$. II. Neutron scattering studies of a cluster type spin glass of $90FeTiO_{3\,10}Fe_2O_3$. J Phys Soc Jpn 54:781

Arai M, Ishkawa Y, Takei H (1985) A new oxide spin glass system of $(1 - x)FeTiO_3 x Fe_2O_3$. IV. Neutron scattering studies on a reentrant spin glass of $79FeTiO_3 21Fe_2O_3$ single crystal. J Phys Soc Jpn 54:2279

Binder K, Young AP (1984) Logarithmic dynamic scaling in spin-glasses. Phys Rev B 29:2864

Burton BP, Robinson P, McEnroe SA, Fabian K, Ballaran TB (2008) A low-temperature phase diagram for ilmenite-rich compositions in the system Fe_2O_3–$FeTiO_3$. Am Mineral 93:1260

Charilaou M, Löffler JF, Gehring AU (2011) Fe–Ti–O exchange at high temperature and thermal hysteresis. Geophys J Int 185:647

Charilaou M, Löffler JF, Gehring AU (2011) Slow dynamics and field-induced transitions in a mixed-valence oxide solid solution. Phys Rev B 83:224414

Djurberg C, Svedlindh P, Nordblad P, Hansen MF, Bødker M, Mørup S (1997) Dynamics of an interacting particle system: evidence of critical slowing down. Phys Rev Lett 79:5154

Engelmann R, Kontny A, Lattard D (2010) Low temperature magnetism of synthetic Fe–Ti oxide assemblages. J Geophys Res 115:B12107

Frandsen C, Burton BP, Rasmussen HK, McEnroe SA, Mørup S (2010) Magnetic clusters in ilmenite-hematite solid solutions. Phys Rev B 81:224423

Gehring AU, Guggenberger G, Zech W, Luster J (1997) Combined magnetic, spectroscopic and analytical-chemical approach to infer genetic information for a vertisol. Soil Sci Soc Am J 61:75–78

Gehring AU, Fischer H, Schill E, Granwehr J, Luster J (2007) The dynamics of magnetic ordering in a natural hemo-ilmenite solid solution. Geophys J Int 169:917

Gehring AU, Mastrogiacomo G, Fischer H, Weidler PG, Müller E, Luster J (2008) Magnetic metastability in natural hemo-ilmenite solid solution ($y \approx 0.83$). J Magn Magn Mater 320:3307

Harrison RJ (2009) Magnetic ordering in the ilmenite-hematite solid solution: a computational study of the low-temperature spin glass region. Geochem Geophy Geosy 10:Q02Z02

Harrison RJ, Redfern SAT, Smith RI (2000) In-situ study of the $R\bar{3}$ to $R\bar{3}$c phase transition in the ilmenite-hematite solid solution using time-of-flight neutron powder diffraction. Am Mineral 85:194

Hohenberg PC, Halperin PI (1977) Theory of dynamic critical phenomena. Rev Mod Phys 49:435

Ishikawa Y (1962) Magnetic properties of ilmenite-hematite system at low temperature. J Phys Soc Jpn 12:1835

Ishikawa Y, Arai M, Saito N, Kohgi M, Takei H (1983) Spin glass properties and magnetic correlation in $FeTiO_3$–Fe_2O_3 system. J Magn Magn Mater 31:1381

Ishikawa Y, Saito N, Arai M, Watanabe Y, Takei H (1985) A new oxide spin glass system of $(1 - x)FeTiO_3$–$(x)Fe_2O_3$. I. Magnetic properties. J Phys Soc Jpn 54:312

Lindsley DH (1963) Fe–Ti oxides in rocks as thermometers and oxygen barometers. Carnegie Inst Wash Yearb 62:60

Mauger A, Ferrè J, Ayadi M, Nordblad P (1988) Dynamics of the spin-glass freezing in $Cd_0.6Mn_0.4Te$. Phys Rev B 37:9022

McEnroe SA, Carter-Stiglitz B, Harrison RJ, Robinsom P, Fabian K, McCammon C (2007) Magnetic exchange bias of more than 1 Tesla in a natural mineral intergrowth. Nat Nanotechnol 2:631

Ogielski AT, Morgenstern I (1985) Critical behavior of three-dimensional ising spin-glass model. Phys Rev Lett 54:928

Rüdt C, Jensen PJ, Scherz A, Lindner J, Poulopoulos P, Baberschke K (2004) Higher harmonics of the *ac* susceptibility: analysis of hysteresis effects in ultrathin ferromagnets. Phys Rev B 69:P014419

Sauerzapf U, Lattard D, Burchard M, Engelmann R (2008) The titanomagnetite/ilmenite equilibrium: new experimental data and thermooxybarometric application to the crystallization of basic to intermediate rocks. J Petrol 49:1161–1185

Souletie J, Tholence JL (1985) Critical slowing down in spin glasses and other glasses: fulcher versus power law. Phys Rev B 32:516